Effects of Computer Vision-Monitored Variable Temperature Drying on Drying Kinetics and Quality Attributes of Potato Slices

Xin Xu[a], Jian-Bo Liu[b,*], Tian-Jian Zhang[b], Qing Xu[a], Zhong-Hua Wu[a]

[a.] *Tianjin Key Laboratory of Integrated Design and On-Line Monitoring for Light Industry and Food Machinery and Equipment, College of Mechanical Engineering, Tianjin University of Science and Technology, No. 29, 13th Street, Binhai New Area, Tianjin, 300222, China;*

[b.] *College of Engineering and Technology, Tianjin Agricultural University, No. 22, Jinjing Road, Xiqing District, Tianjin, 300392, China;*

ABSTRACT

Conventional drying overlooks the distinct characteristics of different drying stages, while empirical models possess inherent limitations that prevent them from accurately reflecting the actual drying state of the material. This often leads to prolonged drying times, low efficiency, and poor product quality. This study proposes an intelligent drying apparatus based on computer vision detection, enabling real-time acquisition and measurement of images, mass, and temperature. This capability allows for the implementation of tailored drying strategies at different drying stages. Potato slices were subjected to drying using hot air drying (HAD) at constant temperatures and computer vision-monitored variable temperature drying (CVTD). The effects of these methods on drying kinetics, color, rehydration ratio, specific energy consumption (SEC), and microstructure were investigated. The experimental results demonstrate that CVTD and 80°C-HAD achieved the shortest drying times. Furthermore, the effective moisture diffusivity (Deff) during the Deceleration of the second stage was higher for CVTD than for 60°C-HAD. Compared to constant-temperature drying, CVTD exhibited superior rehydration capacity, brighter color, and lower specific energy consumption (SEC), and a more porous microstructure conducive to moisture migration. These findings collectively indicate that CVTD is a highly promising approach for the drying of potato slices.

KEYWORDS

potato slices; drying kinetics; physicochemical properties; computer vision-monitored variable temperature Drying (CVTD)

1. Introduction

Driven by heightened national awareness of food safety and nutrition, the quality and preservation of food products have emerged as a significant research focus.[1] Attributes such as shelf life, visual appearance, and nutritional content are increasingly prioritized by consumers and producers alike. However, agricultural produce, characterized by high moisture content, is highly susceptible to spoilage and deterioration. This vulnerability leads to substantial postharvest losses, estimated at approximately 30% annually for fruits and vegetables in many developing regions (e.g., South Africa), incurring significant economic costs.[2] Food loss and waste (FLW) has consequently escalated into a critical global challenge.[3] As shown in Fig. 1a, the India Food Corporation reported annual wastage of agricultural produce valued at 58 billion rupees in the country. Similarly, the African Postharvest Losses Information System estimated that 18% of Ghana's maize is lost due to inadequate postharvest storage practices, resulting in

Contact: Prof. Jian-Bo Liu, qingzhoujianbo@126.com, College of Engineering and Technology, Tianjin Agricultural University, Tianjin, 300392, China

economic losses of USD 134 million.[4] In the United States, losses at the farm level may range from 15% to 35%, translating to an annual economic cost between USD 90 billion and USD 100 billion.[5] Moreover, in China, fruits and vegetables account for a substantial 62% of the total FLW.[6] Such significant wastage results in considerable losses of both energy resources and economic value.[7]

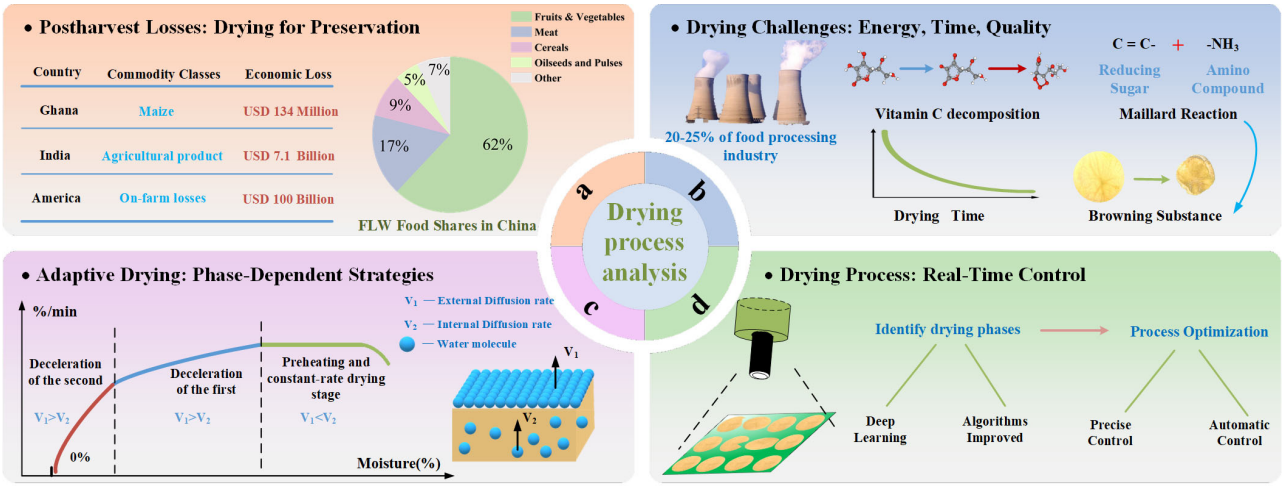


Figure 1. Drying process analysis. (a). postharvest: drying for preservation. (b). drying challenges: energy, time, quality. (c). adaptive drying: phase-dependent strategies. (d). drying process: real-time control.

Drying serves as a prevalent and essential processing method for shelf-life extension. By reducing the material's water content, it effectively suppresses microbial activity, thereby prolonging storage duration.[8] As an indispensable processing step for the safe storage of agricultural products, drying plays a critical role in enhancing food safety. Within the realm of food processing, this technology necessitates a balanced consideration not only of energy efficiency and economic viability but also of key quality attributes, including flavor profile, visual texture, color retention, rehydration capacity, and nutrient preservation. This holistic approach is fundamental to producing high-quality dried products.[9-10] As shown in Fig.1b, drying represents an energy-intensive unit operation within industrial processes. Its energy consumption accounts for 20%–25% of total energy usage in food processing. Notably, drying is also extensively employed across other industrial sectors. Critically, studies indicate that a mere 1% reduction in drying energy consumption may yield up to a 10% increase in operational profits. [11-12] Analysis by Santos et al. [13] demonstrated that ascorbic acid (vitamin C) undergoes degradation during drying, initially decomposing into dehydroascorbic acid, which is subsequently oxidized to 2,3-diketogulonic acid. This reaction pathway results in significant nutrient depletion. Furthermore, the Maillard reaction contributes to the browning of dried products.[14] Analysis of drying kinetics and moisture migration principles reveals distinct stages, as shown in Fig.1c. During the preheating and constant-rate drying stages, the external diffusion rate V_1 is lower than the internal diffusion rate V_2 [15] Consequently, the drying rate remains relatively constant and is predominantly governed by external environmental conditions. When $V_1>V_2$, the process transitions into the falling-rate drying period, encompassing both the first and second falling-rate sub-stages. At this point, a desiccated

crust forms on the material surface. This crust development not only induces surface hardening but also significantly increases the resistance to internal moisture migration towards the exterior.[16] The drying rate in this stage is primarily dictated by the internal diffusion rate of the material. However, it simultaneously presents challenges related to elevated energy consumption and degradation of product quality.

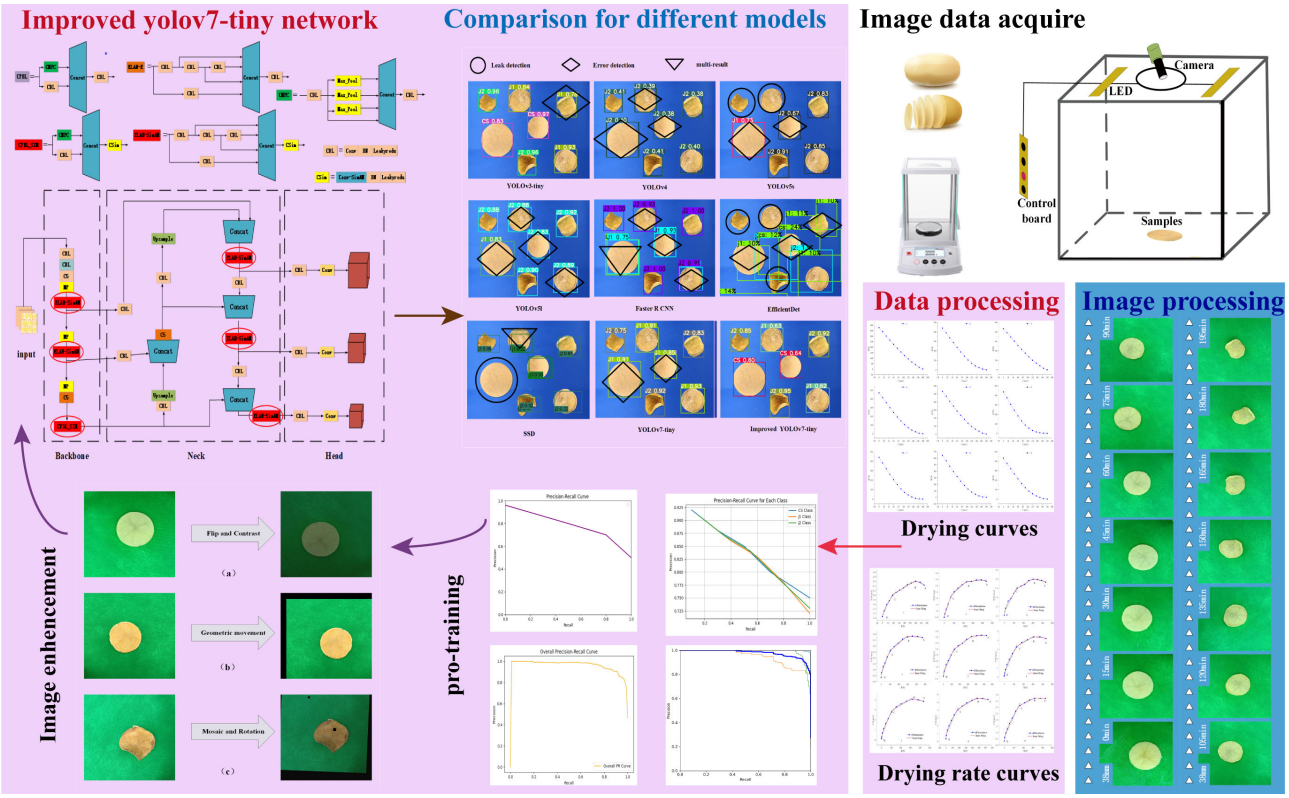


Figure 2. Computer Vision-Monitored Drying Stage Identification. [18]

Employing non-destructive monitoring techniques to oversee the drying process and implement stage-specific drying strategies represents a promising approach.[17] As shown in Fig. 1d, utilizing computer vision technology to identify the current drying stage for subsequent process optimization constitutes a viable strategy. This monitoring process involves tasks related to deep learning and model refinement. In our prior research,[18] we developed an optimal model for identifying drying stages of potato slices. As shown in Fig. 2, this model was derived through a sequence of steps involving image acquisition during potato drying, collection and processing of mass data, model pre-training and screening, and model enhancement. The refined YOLOv7-tiny model ultimately demonstrated superior performance.

Therefore, under the premise of real-time acquisition of drying status, implementing distinct drying conditions tailored to specific drying stages constitutes a viable strategy, termed Computer Vision-Assisted Variable Temperature Drying (CVTD). Specifically, an elevated drying temperature is applied during the constant-rate period. Subsequently, the drying temperature is reduced upon entering the first falling-rate sub-stage, and further minimized during the second falling-rate sub-stage. The primary objective of this study is to investigate the effects of CVTD on the drying characteristics, physicochemical properties, and microstructure of potato slices. Additionally, the intercorrelations among various quality attributes of the dried product are analyzed.

2. Materials and methods

2.1 Materials

Potato served as the experimental material in this study. Approximately 50 fresh yellow-fleshed potatoes with uniform texture, free from mechanical damage, insect infestation, and exhibiting freshness, were procured from a local supermarket in Tianjin. Prior to experimentation, the samples underwent thorough washing with deionized water. Subsequently, the potatoes were sliced into specimens with a diameter of 38 mm and a thickness of 5 ± 1 mm using a slicer and a circular cutter.

The initial moisture content of potatoes was 83.82% (in wet basis), which was determined by vacuum drying at 70 °C for 24 h following the AOAC standard method. [19]

2.2 Experimental System

As shown in Fig. 3, the computer vision-assisted hot air drying system comprises the following components: an experimental bench, a hot air drying chamber (Li-Chen Scientific Instruments, Hunan, China), an industrial camera, an LED illumination source, a fiber optic temperature transmitter, an electronic balance (Li-Chen Scientific Instruments, Hunan, China), a computer, and drying stage identification software. The drying stage identification software incorporates an improved YOLOv7-tiny model [18] encapsulated within a PyQt5 framework. This system processes images captured by the industrial camera in real-time to directly determine the drying stage of potato slices (i.e., constant-rate period, first falling-rate substage, and second falling-rate substage). An automated weighing system — comprising an electronic balance and a polytetrafluoroethylene (PTFE) sample stage — acquires potato mass data in real-time with an accuracy of ±0.01 g. Images are acquired through a dedicated optical port located atop the drying chamber. This port is sealed with heat-resistant quartz glass, effectively isolating the chamber interior from the external environment. Supplementary illumination is provided by an LED source directed through the drying chamber's existing viewport.

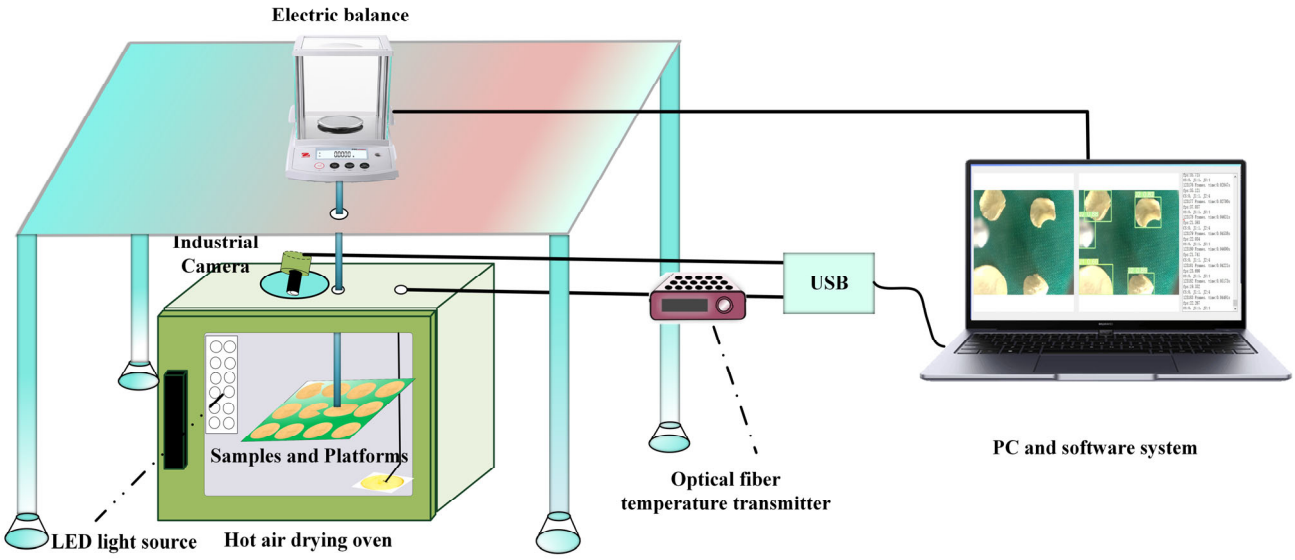


Figure 3. Computer vision-assisted hot air drying system.

2.3 Drying methods

In this study, conventional hot air drying (HAD) and computer vision-assisted variable temperature drying (CVTD) were applied to dehydrate potato slices at distinct temperature regimes. To achieve thermal equilibrium, the drying chambers were preheated for 15 minutes prior to the commencement of drying experiments.

Drying trials were performed using the aforementioned system. Three discrete temperature levels (80°C, 70°C, and 60°C) were established for conventional HAD treatments. Sample mass was recorded at 10-minute intervals. Measurements continued until the drying endpoint was attained, which was defined as the time when the mass change of the sample was less than 0.01 g over a 10-minute interval (equivalent to a moisture content of below 10% wet basis). CVTD drying trials were conducted using the aforementioned system. The drying stage was dynamically determined by the computer vision recognition system. An elevated temperature of 80°C was applied during the preheating and constant-rate period. The temperature was reduced to 70°C in the first falling-rate substage. A minimized temperature of 60°C was maintained in the second falling-rate substage. Sample mass was recorded at 10-minute intervals. Measurements terminated upon reaching the drying endpoint.

Computer vision monitoring has been successfully implemented across diverse process identification and monitoring scenarios, demonstrating notable efficacy in industrial settings. Yu Y et al. [20] implemented an automated detection system for multiple defect types in potatoes using YOLOv3-tiny, including but not limited to sprouting, common scab, insect holes, dry rot, and bruises. Therefore, the primary objective of this study is to investigate the effects of conventional HAD and CVTD under distinct temperature conditions on four critical parameters of potato slices: drying characteristics, color properties, rehydration behavior, and energy consumption.

2.4 Drying characteristics analysis

2.4.1. Drying Rate and Moisture ratio

The moisture ratio (MR) and the dry basis moisture content of potato slices was calculated according to Eq. (1) and Eq. (2), and the drying rate was calculated as shown in Eq. (3): [21-22]

$$MR = \frac{M_t}{M_0} \tag{1}$$

$$M_t = \frac{m_i - m}{m} \times 100\% \tag{2}$$

where, M_0 is the initial moisture content of the potato sample, g/g (dry basis); M_t is the moisture content of the sample at t time, g/g (dry basis). m is the absolute quality, g； and m_i is the mass at moment i, g.

$$U = -\frac{\mathrm{d}Mt}{dt} \tag{3}$$

Where U is the drying rate, %/min； and t is time, min. Moisture ratio (MR) and time (t) relationship curve is called the drying curve, and the relationship curve between drying rate (U) and moisture content (M_t) is called the drying rate curve.

2.4.2 Effective moisture diffusivity (D_{eff})

Eq. (4) was used to calculate the effective moisture diffusivity (D_{eff}) during the drying process of potato slices, according to Fick's law.[23-24]

$$\ln MR = \ln\left(\frac{8}{\pi^2}\right) - \left(\frac{\pi^2 D_{\mathrm{eff}}}{H^2}\right) t \tag{4}$$

where D_{eff} indicates the effective moisture

Contact: Prof. Jian-Bo Liu, qingzhoujianbo@126.com, College of Engineering and Technology, Tianjin Agricultural University, Tianjin, 300392, China

diffusivity, m^2/s; H notes the thickness of potato slices with 0.0050 m; t is the drying time for drying process, s. The slope k is determined by the relationship between *MR* and t, as shown in Eq. (5).

$$k = \frac{\pi^2 D_{\text{eff}}}{H^2} \tag{5}$$

2.4.3 Activation energy (Ea)

The Arrhenius equation demonstrates the relationship between drying activation energy (*Ea*) and D_{eff}, from which Eq. (6) was used to further calculate the Ea. In the given equation, D_0 represents the basis of effective moisture diffusivity in the sample at 273.15 K, m2/s, while Ea represents the activation energy of drying, J/mol. R is the molar gas constant (8.314 J/(mol K)) and *T* indicates the set drying temperature, °C.

$$D_{\text{eff}} = D_0 \exp\left[-\frac{E_a}{R(T+273.15)}\right] \tag{6}$$

Eq. (7) is derived by taking the logarithm of both sides of Eq. (5). The value of Ea is calculated from the slope of the linear relationship between lnDeff and 1/(*T*+273.15), which is represented by ($-E_a/R$).

$$\ln D_{\text{eff}} = \ln D_0 - \frac{E_a}{R}\frac{1}{(T+273.15)} \tag{7}$$

2.5 Rehydration ratio

The rehydration ratio (*Rr*) is a critical evaluation index characterizing the ability of dried fruits and vegetables to absorb water and regain freshness.

Dried potato slice samples were immersed in a constant-temperature water bath at 80°C for 3 hours. Rehydrated slices were then placed on clean filter paper to absorb surface moisture. Samples were equilibrated for 30 minutes prior to weight measurement. And the *Rr* was determined using Eq. (8): [25]

$$Rr = \frac{m_2}{m_1} \tag{8}$$

where *Rr* is the rehydration ratio, g/g; m_2 is the sample mass after rehydration, g; m_1 is the sample mass before rehydration, g.

The dried potato cubes were ground into powder and then its colorimetric values (*L**, *a**, *b**) were measured using a colorometer (SMY-2000SF, Shengmingyang Co., Beijing, China) according to CIELAB color system. The total color difference (Δ*E)* between the dried and the raw samples was evaluated by Eq. (5).

2.6 Color measurement

In order to ensure chromameter accuracy, the rehydrated potato slices were measured. Color parameters (L, a, b*) were quantified using a chromameter (DS-700D, Caipukeji Co., Taizhou, China) based on the CIELAB system. Total color difference (ΔE) between rehydrated and raw samples was calculated with Eq. (9): [26]

$$\Delta E = \sqrt{(L^* - L_0^*)^2 + (a^* - a_0^*)^2 + (b^* - b_0^*)^2} \tag{9}$$

where L_0^*, a_0^*, and b_0^* represent the lightness, greenness/redness, and blueness/yellowness of the fresh potato samples after vacuum freezing, respectively, while the L^*, a^*, and b^* represent the color parameters of the dried samples, respectively.

2.7 Specific energy consumption (SEC)

In order to enhance energy consumption accuracy for each drying process, the specific energy consumption (SEC) was measured during all drying trials. SEC was calculated using Eq. (10): [27]

$$\text{SEC} = \frac{1000W}{m_0\varphi_0 - m_i\varphi_i} \tag{10}$$

where, W is the energy consumed before and after the experiment (measured by ammeter), kW•h; m_0 and m_i are the initial and final masses of the materials, g; φ_i represents the moisture content (wet basis) at the end of the drying and φ_0 indicates the initial moisture content (wet basis), %.

2.8 Microstructure by Scanning Electron Microscopy (SEM)

The dried potato cubes were observed by a scanning electron microscopy (SU3500, Hitachi, Japan). Samples were sprayed with gold for 120s and observed at × 500 and × 1000 magnifications with an accelerating voltage of 15.0 kV × 6.0mm.

2.9 Statistical analyses

The experimental data which were expressed as the mean of three determinations ± standard deviation, were analyzed by ANOVA and Duncan's multiple range test using SPSS statistics software (Version 21.0, SPSS Inc., Chicago, IL, USA) at α=0.05 level. Correlation analysis was executed with the OmicStudio tool [28] https://www.omicstudio.cn/tool.

3. Results and discussion

3.1 Drying characteristics

3.1.1. Drying kinetics curves

During the initial drying phase (Preheating and constant-rate drying stage), potato slices are enveloped by a surface liquid film. The drying rate is primarily governed by the external diffusion rate (V_2) [15], which increases with rising temperatures. Thus, employing higher temperatures significantly accelerates drying while minimally affecting product quality. Upon entering deceleration of the first stage, the Internal diffusion rate becomes rate-limiting as the surface desiccates. Temperature reduction is essential here to prevent surface hardening and quality deterioration caused by overheating. In deceleration of the second, both free water and bound water are largely removed from the material. Maintaining high temperatures would damage cellular pathways, impeding internal moisture transfer. Therefore, further temperature reduction is required. The Computer Vision-Monitored Variable Temperature Drying (CVTD) strategy implemented in this study applies:

- 80°C during Preheating and constant-rate drying stage.
- 70°C in Deceleration of the first stage.
- 60°C in Deceleration of the second stage.

The effects of hot air drying temperature and CVTD on the drying curves of potato slices are shown in Fig. 4A. It can be seen that significant differences exist in the drying kinetics among the different drying methods. When the HAD temperature increased from 60°C to 80°C, the total drying time decreased from 130 min to 100 min. This conforms to the general principles of hot air drying [29]. The total drying time for CVTD was 103 min. Compared to 60°C-HAD, this represents a reduction of 20.78% in drying time, while compared to 70°C-HAD, it represents a reduction of 6.36%. Its drying time was close to that of 80°C-HAD.

Specifically, Fig. 4D shows the duration of CVTD in different drying stages. The Preheating and constant-rate drying stage (at 80°C) lasted only 18 min, the Deceleration of the first stage (at 70°C) lasted 35 min, and the Deceleration of the second stage (at 60°C) had the longest duration, reaching 50 min.

Throughout the entire CVTD process, the ambient temperature was maintained at 80°C for only 18 min, yet the final drying time was close to that of 80°C-HAD. This fully demonstrates the superiority of CVTD.

3.1.2 Drying rate

Fig. 4B reflects the drying rate curves of

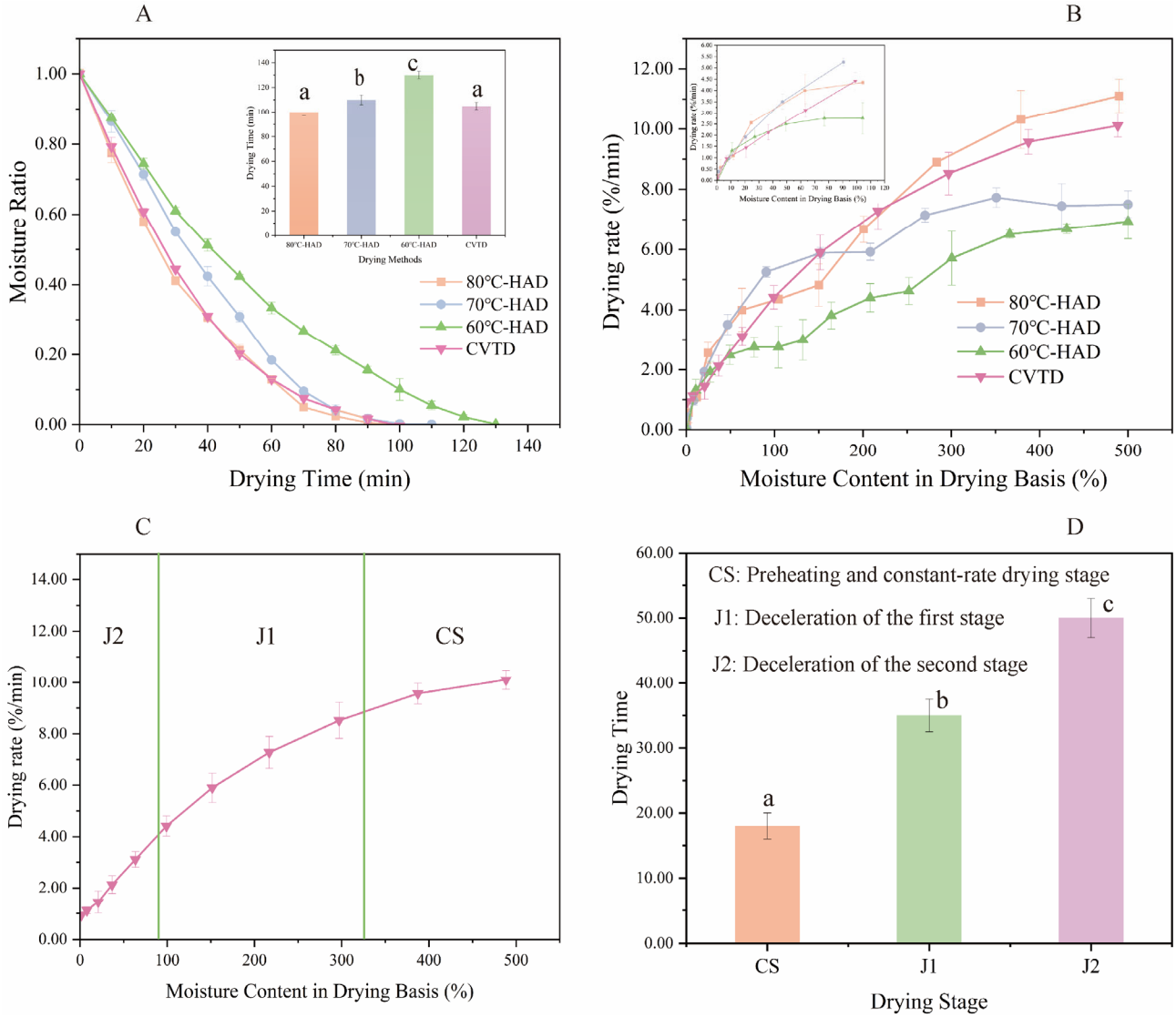


Figure 4. Drying characteristics of potato slices under different drying conditions. A. Drying curves. B. Drying rate curves. C. CVTD drying rate curve. D. Stage Duration in CVTD Drying

constant-temperature hot air drying at different temperatures and CVTD. The experimental results indicate that as the moisture content decreased, the drying rate initially maintained a relatively high level, followed by a rapid decline. After passing a certain point, the rate of decrease accelerated. [18] The drying process of the potato slices underwent the preheating and constant-rate drying stage, the Deceleration of the first stage, and the Deceleration of the second stage. Figs. 4C and 4D reflect the temperature transition points and the time durations for each drying stage in CVTD. Evidently, the Deceleration of the second stage required the longest time, while the preheating and constant-rate drying stage was the shortest. This conforms to the general principles of the drying process.

The drying rate of CVTD during its initial phase (Preheating and constant-rate drying stage) was significantly higher than that of constant-

temperature drying at 70°C and 60°C. This is attributed to the 80°C condition employed during the Preheating and constant-rate drying stage of CVTD (0~18 min). As drying progressed into the Deceleration of the first stage (18~53 min), the drying temperature decreased to 70°C, causing a rapid decline in the CVTD drying rate. Around 50 min, it intersected with the drying rate of 70°C-HAD and subsequently remained lower. Upon entering the Deceleration of the second stage (53~103 min), the drying temperature was reduced to 60°C. Although the drying rate continued to decline, it remained higher than that of 60°C-HAD. This could be attributed to the timely reduction in drying temperature during the Deceleration of the first stage, which prevented significant thermal hardening on the surface of the potato slices and resulted in less collapse of intracellular pathways. [30-31] Consequently, internal moisture migration was not substantially impeded. Concurrently, the formation of a loose and porous structure facilitated moisture migration, thereby leading to a significantly higher drying rate in the later stage compared to 60°C-HAD.

3.1.3 Effective moisture diffusivity (D_{eff}) and activation energy (E_a)

Table 1 displays the Deff values of potato slices under constant-temperature drying at different temperatures and CVTD. As the drying temperature increased (from 60 to 80°C), the Deff of the potato slices rose from 1.165×10^{-9} m²/s to 2.454×10^{-9} m²/s. A similar trend was observed in the HAD drying of goji berries (Lycium barbarum)[32], which is likely due to the higher temperature providing additional energy. This increased the kinetic energy of water molecules, thereby enhancing their mobility and promoting moisture migration.

Although the ambient temperature during the J2 stage of CVTD was consistent with that of 60°C-HAD, the Deff value (2.191×10^{-9} m²/s) was higher than that of 60°C-HAD (1.165×10^{-9} m²/s). This is likely because the variable-temperature treatment applied in the earlier stages of CVTD altered the microstructure of the material, significantly reducing the moisture diffusion resistance and enhancing the diffusion efficiency during the J2 stage.

Table 1. Effective moisture diffusion coefficients and activation energy.

Parameter	Conditon	Linear regession equatioin	R^2	D_{eff} (10^{-9}m²/s)	E_a(kJ/mol)
	80	$\ln MR = -9.69 \times 10^{-4} t + 0.034$	0.978	2.454	
HAD	70	$\ln MR = -8.69 \times 10^{-4} t + 0.011$	0.986	2.201	45.53
	60	$\ln MR = -4.60 \times 10^{-4} t - 0.080$	0.992	1.165	
	CS	$\ln MR = -4.28 \times 10^{-4} t - 0.001$	0.995	1.084	
CVTD	J1	$\ln MR = -6.40 \times 10^{-4} t + 0.244$	0.992	1.621	34.21*
	J2	$\ln MR = -8.65 \times 10^{-4} t + 1.992$	0.970	2.191	

E_a reflects the difficulty of drying the material and can be used to estimate the energy consumption required for drying.[33] Research indicates that the drying activation energy (E_a) for agricultural materials typically falls within the range of 12.7 to 111.0 kJ/mol. As shown in Table 1, the E_a for potato slices dried by HAD was 45.53 kJ/mol. This indicates that removing 1 mol of bound water molecules from potato slices via HAD requires 45.53 kJ. Conversely, under CVTD drying, the calculated E_a was 34.21 kJ/mol, suggesting that removing 1 mol of bound water molecules from potato slices via CVTD requires only 34.21 kJ.

3.2 Color analysis

Color is a primary sensory indicator for potato slices. Table 2 presents the color parameters of samples rehydrated under different drying conditions. The fresh sample exhibited L, a, and b values of 60.01, -1.44, and 6.14, respectively. Compared to the fresh sample, samples rehydrated after 80°C-HAD and 70°C-HAD showed a significant increase ($P < 0.05$) in L* and b* values. Conversely, samples rehydrated after 60°C-HAD and CVTD exhibited a significant decrease ($P < 0.05$) in L* and b* values. A significant increase ($P < 0.05$) in a* value was observed for samples rehydrated after 80°C-HAD and 60°C-HAD compared to the fresh sample, indicating a shift towards red. In contrast, samples rehydrated after 70°C-HAD and CVTD showed a significant decrease ($P < 0.05$) in a* value compared to the fresh sample. This reduction could be attributed to prolonged oxygen exposure during drying, leading to oxidation [33]. The results indicate that the CVTD sample achieved a lower ΔE value after rehydration, suggesting that employing strategic temperature variations during different drying stages yields potato slices with superior color characteristics.

Table 2. Effects of different drying techniques on color and energy consumption of potato cubes.

Drying methods	***Color parameters***				***Energy consumption*** (kW•h/kg)
	L*	***a****	***b****	***ΔE***	
Fresh	60.01±0.02^{c}	-1.44±0.23^{c}	13.32±0.04^{c}	—	—
80°C-HAD	65.15±0.33^{b}	-0.5±0.12^{b}	22.06±0.34^{a}	10.18±0.18^{b}	9.82
70°C-HAD	69.53±0.05^{a}	-1.85±0.32^{bc}	16.96±0.06^{b}	10.21±0.05^{b}	9.23
60°C-HAD	48.51±0.11^{e}	1.13±0.08^{a}	10.78±0.15^{c}	12.04±0.05^{c}	7.14
CVTD	53.74±0.18^{d}	-2.63±0.04^{d}	8.50±0.43^{d}	8.26±0.41^{a}	6.47

3.3 Rehydration ratio

During the drying process, the tissue structure of the material undergoes changes, significantly impacting its rehydration capacity. As shown in Fig. 5A, the *Rr* values for samples dried by 80°C-HAD and 70°C-HAD were 3.90 and 4.21, respectively, with no significant

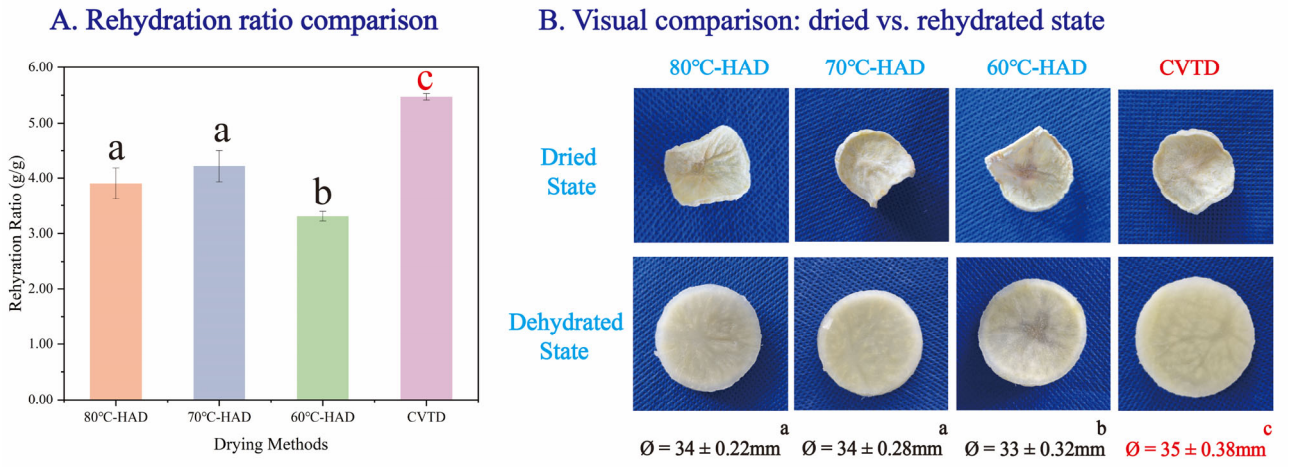


Figure 5. Effect of different drying methods on rehydration ratio. A. Rehydration ratio comparison. B. Visual comparison: dried vs. rehydrated state.

difference between them. The sample dried by 60° C-HAD exhibited the poorest rehydration capacity, with an *Rr* value of 3.42. This is likely attributable to the slow moisture migration rate during low-temperature drying, which promoted the formation of a dense structure detrimental to rehydration. Conversely, the CVTD sample demonstrated the optimal rehydration capacity, achieving an *Rr* value of 5.47, which was significantly higher ($P < 0.01$) than those of all other drying groups.

Fig. 5B presents photographs of potato slices dried by 80° C-HAD, 70° C-HAD, 60° C-HAD, and CVTD, both in the dried state and after rehydration. The results show that the 60° C-HAD sample exhibited the darkest color, consistent with the analysis in Section 3.2 (Color analysis). Furthermore, the rehydrated CVTD potato slice reached a diameter of 35 mm, significantly larger than those of the 80° C-HAD, 70° C-HAD, and 60° C-HAD samples. This superior performance could be attributed to the CVTD drying strategy altering the internal structure of the potato slices [34], resulting in a loose, porous structure that facilitates rehydration capacity. This interpretation is strongly supported by the SEM observations (Section 3.5), which revealed a well-formed porous network in CVTD samples, in contrast to the dense and collapsed structures found in HAD samples.

3.4 Specific energy consumption (SEC)

Drying is one of the most energy-intensive industrial operations, accounting for 20% to 25% of total energy consumption in the food processing industry [1]. Consequently, energy consumption is a crucial indicator for the comprehensive evaluation of different drying technologies. The specific energy consumption (SEC) values for potato slices dried under 80° C-HAD, 70° C-HAD, 60° C-HAD, and CVTD

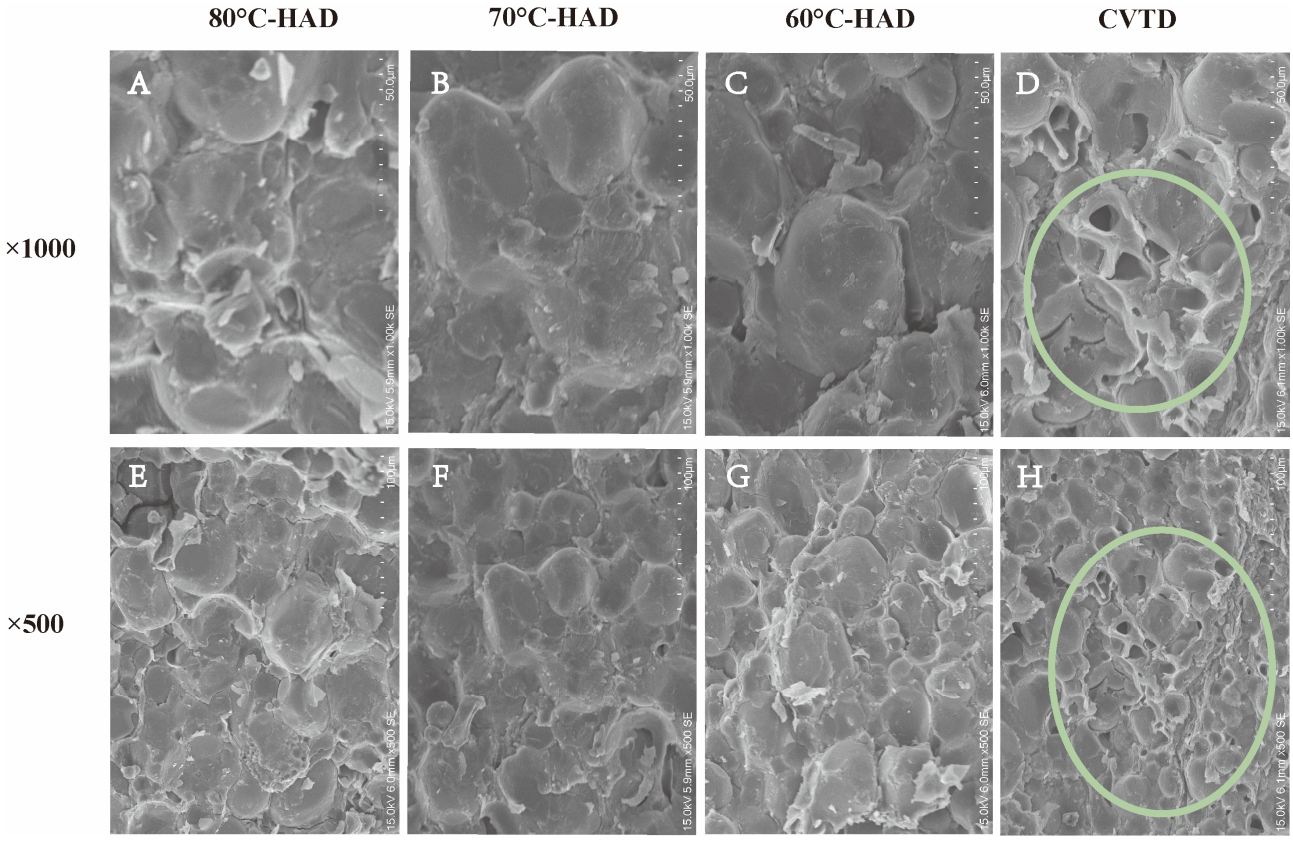


Figure 6. Microstucture observation of potato samples under different drying methods.

Contact: Prof. Jian-Bo Liu, qingzhoujianbo@126.com, College of Engineering and Technology, Tianjin Agricultural University, Tianjin, 300392, China

were 9.82, 9.63, 7.14, and 6.47 kWh/kg, respectively. CVTD exhibited the lowest SEC, which is directly attributable to its shorter drying time. Furthermore, the unique structure formed during CVTD drying facilitates moisture migration more effectively, representing another key factor contributing to its reduced SEC value. This finding aligns with and corroborates the earlier analysis of activation energy (Ea).

3.5 Microstructure changes

Understanding the microscopic structure can elucidate the changes in the material at the cellular level, thereby providing insights into its drying behavior. [35]

To investigate the effect of drying methods on the microstructure of potato slices, scanning electron microscopy (SEM) images of the dried samples were acquired, as shown in Fig. 6. SEM observations revealed that potato slices subjected to constant-temperature HAD treatments developed a dense structure. Both 80°C-HAD and 60°C-HAD samples exhibited varying degrees of cell rupture and starch gelatinization. This can be attributed to the excessive heat generated under the 80°C-HAD condition, which led to the collapse of the cellular structure due to thermal stress. Conversely, the prolonged drying time required for 60°C-HAD also resulted in damage to the cell walls.



Figure 7. Correlation analysis among the rehydration ratio (Rr), color (including L*, a*, b*, and ΔE), Energy

In contrast, the CVTD-treated potato slices maintained relatively intact cellular structures with typically oval-shaped starch granules. Furthermore, the CVTD samples developed a porous structure, as evident in Fig. 6D and Fig. 6H. This advantageous microstructure is a direct result of the stage-specific drying strategies employed by CVTD. The application of a milder drying temperature (60°C) during the Deceleration of the second stage prevented overheating and excessive starch gelatinization. This gentle approach provided the necessary conditions and time for the formation of a porous network. This microstructural advantage is consistent with the energy consumption analysis, explaining why CVTD achieved lower energy usage, shorter drying time, and superior rehydration capacity.

3.6 Correlation analysis

Correlation analysis of the experimental data was performed using the OmicStudio tool [28], with the results presented in Fig. 7. A strong negative correlation was observed between the Rehydration Ratio (Rr) and Total Color Difference (ΔE). This indicates that a smaller color difference (ΔE) corresponds to better rehydration capacity. Since rehydration capacity serves as a macro-manifestation of preserved microstructural integrity, this correlation directly links color preservation to microstructural integrity. Furthermore, a strong negative correlation existed between Rr and Energy (Specific Energy Consumption, SEC). This statistical outcome arises because CVTD achieved both extremely low SEC and excellent rehydration performance (high Rr). Conversely, Energy (SEC) and Drying Time exhibited a strong positive correlation, confirming that drying time is the primary determinant of specific energy consumption.

4. Conclusions

This study investigated the effects of hot air drying at different temperatures and computer vision-guided variable temperature drying (CVTD) on the physicochemical properties, drying kinetics, color, and energy consumption ratio of potato slices. Furthermore, an intelligent computer vision-Monitored drying apparatus was developed. The results indicate that the drying method significantly impacts the overall quality of potato slices. Specifically, CVTD proved to be a promising drying method, exhibiting shorter drying time, higher rehydration ratio, improved color, and lower specific energy consumption compared to traditional drying methods. Scanning electron microscopy (SEM) analysis further confirmed that CVTD-treated samples developed a porous microstructure and well-preserved cellular integrity, which directly contributed to the enhanced moisture diffusion, rehydration capacity, and reduced energy consumption. Additionally, the established intelligent drying apparatus accurately identified the drying stage of potato slices (Preheating and constant-rate drying stage, Deceleration of the first stage, or Deceleration of the second) and implemented different drying strategies accordingly in each stage. These findings provide a valuable reference for selecting potato slice drying processes to minimize drying time, reduce energy consumption, and maintain drying quality.

Disclosure statement

Authors declare that this manuscript is original and authors have no known conflict of interest associated with this manuscript. The results reported in this manuscript have not been influenced by any financial support. We have not excluded any individual who satisfied the authorship criteria. We confirm that all the listed

authors have read and approved the content of the manuscript.

Funding

This research is supported by the Development Fund Project for Young Scientific and Technological Talents of Tianjin Agricultural College (Grant No. 2025QNKJ13) and the Natural Science Foundation of Inner Mongolia (Grant No. 2023QN03060).

References:

[1]. Tucker, AC.; Breshnahan, C.; John, S.; Johnson, J. et al. Food (in)security in relation to nutrition (in)security in a national cross-sectional sample of Supplemental Nutrition Assistance Program participants: considerations of an emerging construct. *Am J Clin Nutr.* **2024**, 119(6), 1475–1484. DOI: 10.1016/j.ajcnut.2024.03.020.

[2]. Zeng, SY.; Du, Zl., Lv, WQ.; Li, D.; Su, DB.; Lv, HZ. Experimental study on the hygrothermal dynamics of peanut (Arachis hypogaea Linn.) in the process of superposition and variable temperature drying. *J. Drying Technology,* **2022**, 40(7), 1463–1477. DOI:10.1080/07373937.2021.1873359.

[3]. Aschemann-Witzel, J. Waste not, want not, emit less. *Science*. **2016**, 2016, 352(6284): 408-409. DOI:10.1126/science.aaf2978.

[4]. Adams, F.; Aidoo, R.; Mensah, J.; Mensah, A.; Etuah, S. et al. The synergy between farmers' declaration of qualitative and quantitative maize postharvest losses in the transition agroecological zone of Ghana. *J of Stored Products Research*. **2023**, 104, 102198. DOI:10.1016/j.jspr.2023.102198.

[5]. Deng, L. Z.; Yang, X. H.; Mujumdar, A. S.; Zhao, J. H.; Wang, D.; Zhang, Q.; Wang, J.; Gao, Z. J.; Xiao, H. W. Natural energy materials and storage systems for solar dryers: State of the art. *Solar Energy Materials and Solar Cells,* **2023**, 255:112276. DOI: 10.1016/j.solmat.2023.112276.

[6]. Huang, J. Q. Food Loss and Waste in China: Status Quo, Policies and Actions. *Sino-German Agricultural Centre*. **2021**, https://www.dcz-china.org/2021/12/15/policy-brief-food-loss-and-waste-in-china/

[7]. Kimaro.; Dismas.; Nyangarika.; Anthnoy.; Kivevele.; Thomas. Uncovering Socioeconomic Insights of Solar Dryers for Sustainable Agricultural Product Preservation: A Systematic Review. *Heliyon.* **2024**, 10(23): e40726-e40726. DOI: 10.1016/j.heliyon.2024.e40726

[8]. Mujumdar, A. S.; Xiao, H. W. Advanced Drying Technologies for Foods. CRC Press: New York. **2019**.

[9]. Liu, J. B.; Xu, X.; Zhang, T. J.; Wang, J. C.; Wang, R. F.; Xu. Q. Combined effects of low pressure superheated steam drying and vacuum drying on sugar reduction and quality attribute in mango (Mangifera indica L.) slices. *Int. J. Food Eng*. **2024**, 20(6): 405-417. DOI: 10.1515/ijfe-2023-0249.

[10]. Onwude, D.; Hashim, N.; Chen, G. N. Recent advances of novel thermal combined hot air drying of agricultural crops. *Trends in Food Science & Technology* **2016**, 57: 132-145. DOI: 10.1016/j.tifs.2016.09.012.

[11]. Lamidi, R. O.; Jiang, L.; Pathare, P. B.; Wang, Y. D; Roskilly, A. P. Recent advances in sustainable drying of agricultural produce: A review. *Applied Energy,* **2019**, 233: 367-385. DOI: 10.1016/j.apenergy.2018.10.044.

[12]. Siddiqui, S.; Ucak, I.; Jain, S.; Elsheikh, W.; Redha, A.; Kurt, A. Impact of drying on techno-functional and nutritional properties of food proteins and carbohydrates - A comprehensive review. *Drying Technology*. **2024**, 42(4), 592-611. DOI: 10.1080/07373937.2024.2303580.

[13]. Santos, P. H. S.; Silva, M. A. Retention of Vitamin C in Drying Processes of Fruits and VegetablesA Review. *Drying Technology*. **2008,** 26(12), 1421–1437. DOI: 10.1080/07373930802458911.

[14]. Dai, J. W.; Rao, J. Q.; Wang, D.; Xie, L.; Xiao, H. W.;

Liu, Y. H.; Gao, Z. J. Effect of the ripening stage on the pulsed vacuum drying behavior of goji berry (Lycium barbarum L.): Ultrastructure, drying characteristics, and browning mechanism. *Food Chemistry*. **2024**, 442, 138489. DOI: 10.1016/j.foodchem.2024.138489.

[15]. Ju, H. Y.; Zhao, S. H.; Mujumdar, A. S.; Fang, X. M.; Gao, Z. J.; Zheng, Z. A.; Xiao, H. W. Mass Transfer "Regime" Approach to Drying. *Industrial & Engineering Chemistry Research.* **2021**, 60(26), 9613-9623. DOI: 10.1021/acs.iecr.1c01680.

[16]. Yao, B.; Zhang, X. K.; Wen, X. D. Developments of Variable Temperature Drying Technology for Agricultural Products at Home and Abroad. *Food Sci. Technol.* **2015**, 40, 94–98. DOI: 10.13684/j.cnki.spkj.2015.07.022.

[17]. Rojas, M. L.; Augusto, P. E. Successive Two-Stage Hot Air-Drying with Humidity Control Combined Radio Frequency Drying Improving Drying Efficiency and Nutritional Quality of Amomi fructus. *Food and Bioprocess Technol*. **2023**, 16(1), 149-166. DOI: 10.1007/s11947-022-02928-8.

[18]. Xu, X.; Liu, J. B.; Zhang, T. J.; Wang, R. F; Xu, Q.; et al. Online detection of potato drying stages based on improved YOLOv7-tiny model. *Drying Technology.* **2025**, 43(4), 679-689. DOI: 10.1080/07373937.2025.2450700.

[19]. AOAC. Official Methods of Analysis, 15th ed.; Association of Official Analytical Chemists: Washington, DC, USA, 1990.

[20]. Yang, Y.; Liu, Z. F.; Huang, M.; Zhu, Q. B.; Zhao, X. Automatic detection of multi-type defects on potatoes using multispectral imaging combined with a deep learning model. *Journal of Food Engineering*. **2023**, 336, 111213. DOI: 10.1080/07373937.2018.1494185.

[21]. Chettri, S.; Jena, S.; Nath, P. C.; Rustagi, S.; Katyal, M.; Sharma, R.; Panda, B.; Mohanta, Y. Optimization of vacuum drying characteristics of red and green cherry pepper paste using response surface methodology: a comparative study. *Cogent Food & Agriculture.* **2025**, 11(1), 2481421. DOI: 10.1080/23311932.2025.2481421.

[22]. Faliarizao, N.; Siddiq, M.; Dolan, K. Total phenolics, antioxidant, and physical properties of red chili peppers (Capsicum annum L.) as affected by drying methods. *International Journal of Food Properties.* **2025**, 28(1), 2492823. DOI: 10.1080/10942912.2025.2492823.

[23]. Das, R.; Islam, M.; Saini, P.; Kaduji, G.; Kaur, R.; et al. Finite element modeling of banana slices in convective drying, studies on isotropic shrinkage kinetics using Arbitrary Lagrangian-Eulerian (ALE) approach. *Thermochimica Acta*. **2025**, 749:180024. DOI: 10.1016/j.tca.2025.180024.

[24]. Tepe, F. B.; Tepe, T. K. Improvement of intermittent microwave drying of red peppers: Effect of ethanol and blanching pretreatments on drying behavior, modeling, energy consumption and some quality attributes. *Thermal Science and Engineering Progress*. **2025**, 63, 103734. DOI:10.1007/s13197-013-0941-y.

[25]. Zang, Z.; Zhang, Q.; Huang, X.; Jiang, C.; He, C.; Wan, F. Official Methods of Analysis, 15th ed.; Effect of Ultrasonic Combined with Vacuum Far-infrared on the Drying Characteristics and Physicochemical Quality of Angelica sinensis. *Food and Bioprocess Technology*. **2023**, 16(11), 2455-2470. DOI: 10.1007/s11947-023-03076-3.

[26]. Link, J. V.; Tribuzi, G.; Laurindo, J. Improving quality of dried fruits: A comparison between conductive multi-flash and traditional drying methods. *Lwt-food Science and Technology*. **2017**, 84, 717–725. DOI 10.1016/j.lwt.2017.06.045.

[27]. Lavelli, V.; Sereikaite, J. Kinetic Study of Encapsulated β-Carotene Degradation in Dried Systems: A Review. *Foods.* **2022**, 11(3), 437. DOI: 10.1007/s11947-009-0300-1.

[28]. Lyu, F.; Han, F.; Ge, C.; Mao, W.; Chen, L.; Hu, H.; Chen, G. et al. OmicStudio: A composable bioinformatics cloud platform with real-time feedback that can generate high-quality graphs for publication. *Imeta*. **2023**, 2(1), e85. DOI: 10.1002/imt2.85.

[29]. Zhang, Q.; Wang, B.; Zhang, H.; Lin, R.; Yang, L.; Lv, W. Q.; Xiao, H.W. Effects of microwave-hot air combined drying on the moisture content, physical

properties, flavor, and volatile components of prunes (Prunus domestica L.). *Drying Technology.* **2025**, 43(6), 993-1005. DOI: 10.1080/07373937.2025.2479871.

[30]. Tao, Y.; Sun, D. W.; Górecki, A.; Blaszazak, W.; Lamparski, G.; Effect of drying conditions on the quality of vacuum-microwave dried potato cubes. *J of Food Eng.* **2007**, 81(2), 306-312. DOI: 10.1016/j.jfoodeng.2006.10.028.

[31]. Leeratanarak, N.; Devahastin, S.; Chiewchan, N. Drying kinetics and quality of potato chips undergoing different drying techniques. *Journal of Food Engineering.* **2006**, 77(3), 635-643. DOI: 10.1016/j.jfoodeng.2005.07.022.

[32]. Xie, L.; Mujumdar, A. S.; Fang, X. M.; Wang, J.; Dai, J. W.; Du, Z. L.; Xiao, H. W.; Liu, Y. H.; Gao, Z. J. Far-infrared radiation heating assisted pulsed vacuum drying (FIR-PVD) of wolfberry (Lycium barbarum L.): Effects on drying kinetics and quality attributes. *Food and Bioproducts Processing.* **2017**, 102: 320-331. DOI: 10.1016/j.fbp.2017.01.012.

[33]. Wang, S.Y.; Zhang, Y. Q.; Wei, Q.; Cui, D. Z.; Fu, X. S.; Liu, Z. L.; Zhang, Z. A. Pulsed Vacuum Drying (PVD) of Hawthorn (Crataegus spp.) Slices: Effects on Drying Characteristics and Physicochemical Quality. *Food and Bioprocess Technology*. **2024**, 17(12), 5410–5422. DOI: 10.1007/s11947-024-03447-4.

[34]. Wang, J.; Law, C. L.; Nema, P. K.; Zhao, J. H.; Liu, Z. L.; Deng, L. Z.; Gao, Z. J.; Xiao, H. W. Pulsed vacuum drying enhances drying kinetics and quality of lemon slices. *Journal of Food Engineering.* **2018**, 224, 129-138. DOI: 10.1016/j.jfoodeng.2018.01.002.

[35]. Mowafy, S.; Guo, J.; Lei, D. W.; Liu, Y. H. Application of novel blanching and drying technologies improves the potato drying kinetics and maintains its physicochemical attributes and flour functional properties. *Innovative Food Science and Emerging Technologies.* **2024**, 94, 103648. DOI: 10.1016/j.ifset.2024.103648.